

Chapter 18

A Miniature Vehicle with Extended Aerial and Terrestrial Mobility

Richard J. Bachmann, Ravi Vaidyanathan, Frank J. Boria, James Pluta, Josh Kiihne, Brian K. Taylor, Robert H. Bledsoe, Peter G. Ifju, and Roger D. Quinn

Abstract This chapter describes the design, fabrication, and field testing of a small robot (30.5 cm wingspan and 30.5 cm length) capable of motion in both aerial and terrestrial mediums. The micro-air-land vehicle (MALV) implements abstracted biological inspiration in both flying and walking mechanisms for locomotion and transition between modes of operation. The propeller-driven robot employs an undercambered, chord-wise compliant wing to achieve improved aerial stability over rigid-wing micro-air vehicles (MAVs) of similar size. Flight maneuverability is provided through elevator and rudder control. MALV lands and walks on the ground using an animal-inspired passively compliant wheel-leg running gear that enables the robot to crawl and climb, including surmounting obstacles larger than its own height. Turning is accomplished through differential activation of wheel-legs. The vehicle successfully performs the transition from flight to walking and is able to transition from terrestrial to aerial locomotion by propeller thrust on a smooth horizontal surface or by walking off a vertical surface higher than 6 m. Fabricated of lightweight carbon fiber the ~100 g vehicle is capable of flying, landing, and crawling with a payload exceeding 20% its own mass. To our knowledge MALV is the first successful vehicle at this scale to be capable of both aerial and terrestrial locomotion in real-world terrains and smooth transitions between the two.

R.D. Quinn (✉)

Department of Mechanical and Aerospace Engineering at Case Western Reserve University, Cleveland, USA
e-mail: roger.quinn@case.edu

Video of the robot during field testing may be observed at: <http://faculty.nps.edu/ravi/BioRobotics/Projects.htm>.

18.1 Introduction

Advances in fabrication, sensors, electronics, and power storage have made possible the development of a wide range of small robotic vehicles capable of either aerial or terrestrial locomotion. Furthermore, insights into animal locomotion principles and mechanisms have significantly improved the mobility and stability of these vehicles. For example, the utility and importance of bat-inspired passively compliant wings for fixed wing micro-air vehicles (MAVS) have been demonstrated for aircraft with wingspans as small as 10 cm [1]. Likewise, highly mobile ground vehicles using animal-inspired compliant legs have been constructed with body lengths as short as 9 cm that can run rapidly over obstacles in excess of their own height [2].

This chapter describes the design, fabrication, and testing of a novel small vehicle (dubbed the micro-air-land vehicle (MALV)) that is capable of *both* aerial and terrestrial locomotion. Robot morphology is inspired by neuromechanics in animal locomotion, integrating passive compliance in its wings, joints, and legs, such that it may fly, land, walk on the ground, climb over obstacles, and (in some circumstances) take to the air again all while transmitting sensor feedback. Experimental testing has demonstrated that the robot can be made rugged enough for field deployment and operation. To our knowledge, MALV is the only existing small vehicle capable of powered flight and crawling, climbing obstacles comparable to its height and transitioning between locomotion modes. In the longer term, the design architecture and locomotion mechanisms are expected to lead to a family of vehicles with multiple modes of locomotion that can be scaled to a range

of functions. Applications targeted include surveillance, reconnaissance, exploration, search/rescue, and remote inspection.

18.1.1 Overview and Design Approach

In a biological organism, execution of a desired motion (e.g., locomotion) arises from the interaction of descending commands from the brain with the intrinsic properties of the lower levels of the sensorimotor system, including the mechanical properties of the body. Animal “neuromechanical” systems successfully reject a range of disturbances which could otherwise induce instability or deformation of planned trajectories [3]. The first response to minimize such effects, in particular for higher frequency disturbances such as maintaining posture over varying terrestrial substrates [4] and unexpected gusts in flight [1, 5], is provided by the mechanical properties (e.g., structures, muscles, and tendons) of the organism. In legged locomotion, for example, a fundamental role is played by compliance (i.e., springs and dampers) in joints and structures that store and release energy, reduce impact loads, and stabilize the body [4] in an intrinsic fashion and thus greatly simplify higher level control [6, 7]. Reproduction of the dynamic properties of muscle and the intrinsic response of the entire mechanical system [8] have been an impediment to the successful realization of animal-like robot mobility over a variety of substrates and through different mediums (e.g., air and land). It is these intrinsic properties of the musculoskeletal system which augment neural stabilization of the body of an organism.

Although biological inspiration offers a wealth of promise for robot mobility, many constituent technologies are not at a state of maturity where they may be effectively implemented for small autonomous robots. Existing power, actuation, materials, and other robotic technology have not developed to the point where animal-like neuromechanics may be directly integrated into robotic systems. Given this challenge, the majority of biologically inspired legged and flying robots have been confined to laboratory or limited field demonstrations. A method to surmount this, known as abstracted biological inspiration [9], focuses principally on the delivery of critical performance characteristics to the engineering system. Abstracted biological inspiration

attempts to extract salient biological principles and to implement them using available technologies. This approach founded the basis of the design methodology aimed at delivering capabilities of flight locomotion, crawling locomotion, and transition between each to MALV.

18.1.1.1 Organization of Chapter

The remainder of this section describes past work in flying and crawling robots individually and some of the small body of research in robots with multimodal mobility. Section 18.2 delineates the biologically inspired structures for flight and walking utilized for MALV. Section 18.3 details the specific design process and fabrication of the vehicle, while Sect. 18.4 provides details on the performance characteristics of the robot based on exhaustive system testing in facsimile field operations. Section 18.5 enumerates the conclusions of the research and envisioned future work.

18.1.2 Micro-ground Vehicles

Two major factors remain significant challenges to the deployment and field utility of terrestrial micro-robots. First, the relative size of real-world obstacles (e.g., stairs, gravel, terrain fluctuations) makes movement a daunting task for small robots. For example, RHex [10], at approximately 50 cm in length, is the shortest existing ground robot to our knowledge that can climb standard stairs without jumping [11–13], flying, or using gripping mechanisms on its feet [14, 15]. Second, power source miniaturization has not kept pace with other critical technologies, such as actuation, sensing, and computation.

A wide array of vehicles have been constructed that attest to the difficulty of designing field-deployable terrestrial mobile micro-robots. Khepera robots have a 5 cm wheelbase, onboard power, and an array of sensors [16]. Although they are widely used by group behavior researchers, their 1.4 cm diameter wheels restrict them to operation on very smooth, flat surfaces. Millibots [17] use tracks, but it is not clear that they offer significant advantages since it is difficult

to implement a modern track suspension at this small scale. A small hexapod has been developed by Fukui et al. [18] that runs in a tripod gait using piezoelectric actuators. However, small joint excursions also limit the vehicle to relatively flat surfaces. Birch et al. [19] developed a 7.5 cm long hexapod inspired by the cricket and actuated by McKibben artificial muscles. Though capable of walking using 2 bars of air pressure it has not yet carried its own power supply. Sprawlita [20] is a 16 cm long hexapod that uses a combination of servomotors and air cylinders. Although Sprawlita attains a top speed of 4.5 body lengths per second, which is fast compared to existing robots of similar size, a necessary operating air pressure of 6 bars makes it unlikely that the robot will become autonomous in its current form.

Abstracted biological inspiration has spawned a group of highly mobile robots, called WhegsTM [21] and Mini-WhegsTM [22]. To our knowledge, Mini-WhegsTM is the fastest small terrestrial vehicle that is also capable of surmounting large obstacles relative to its size. Using a single drive motor, the 9 cm long robot attains a speed of 10 body lengths per second and can easily run over 3.5 cm tall obstacles – higher than the top of its body. The more recently developed iSprawl [23] also uses single motor propulsion and benefits from abstracted biological principles. It has run even faster, 15 body lengths per second, although its obstacle climbing ability is more restricted because of the small excursions of its feet.

18.1.3 Micro-air Vehicles (MAVs)

The majority of research to develop practical (non-rotary) winged MAVs can be categorized into three fundamental approaches. The first and most widely used is to configure the airframe as a lifting body or flying wing using conventional propeller-driven thrust in a manner similar to larger aircraft. In this approach, the emphasis is to increase the relative area of the lifting surface while decreasing drag, directly addressing the decrease in the aerodynamic efficiency and putting less emphasis on issues of stability and control. Research groups have used optimized rigid wings and accepted the need for stability augmentation systems or superior pilot skill to deal with intrinsically unsteady behav-

ior. Among the most successful examples of rigid-wing MAVs designed with this approach is Aerovironment's "Black Widow" [24], an electric 15 cm flying wing. Virtually every component on the aircraft is custom built, including a sophisticated gyro-assisted control system. Other successful examples of rigid-wing designs include the "Trochoid" [25] and the "Microstar MAV" [26]. Both of these also have gyro-assisted stabilization systems, without which these lifting bodies would be difficult to control. This approach differs significantly from natural flight: Birds and bats have well-defined wings and a fuselage, and we find no examples of lifting bodies or flying wings in animals that produce thrust and fly for extended periods rather than simply gliding.

The second approach that is being explored for MAV design draws on direct biological inspiration through mimicry of insect- or bird-like beating wings [27–30] (Chaps. 11, 12, 13, 14, 15, 16). Flapping wings can produce both lift and thrust. Researchers have demonstrated flapping wing MAVs that can fly and even hover [31] (Chap. 14) using the "clap and fling" mechanism as described by Ellington [27]. However, these MAVs are susceptible to failure in even light winds and their payload capacity is very small. This approach remains attractive for future work, in particular for low-speed, low-wind applications such as inside buildings.

In a third approach [32–37], the lifting surface is allowed to move and deform passively like animal wings, which leads to more favorable aerodynamic performance in a fluctuating low Reynolds number environment. These findings helped lead to a flexible wing concept, which has been applied by Ifju to successful MAVs over the past 8 years [1, 38–41]. Based upon this abstracted biologically inspired mechanism flight vehicles have been developed that utilize conventional propeller-driven thrust in combination with an adaptive-shape, compliant wing that responds to flight conditions and also develops a stable limit-cycle oscillation during flight.

18.1.4 Multi-mode Mobility

While the aerial and terrestrial vehicles described above represent significant enhancements in their respective fields, their utility is limited by their

dependence on a single locomotion modality. At present, very few robots have been developed that are capable of multiple modes of locomotion, with the majority of work focusing on swimming/crawling robots. One example is Boxybot [42], which uses a vertically oriented tail and two horizontally oriented fins for aquatic propulsion. By reversing the orientation of one or both of the fins, turning moments or reverse thrust can be generated. Continuous rotation of the fins produces a sort of “pronking” terrestrial movement. A watertight version of RHex [43] has also been equipped with fin-like legs that allow it to swim under water. The neuromechanical design of a more recent amphibious robot is based upon salamanders and it can run on land and swim using the same central pattern generator [44]. To the knowledge of the authors, there are few published works with the stated goal of *both aerial and terrestrial locomotion*. The Entomopter [45] uses reciprocating chemical muscle [46] to produce flapping motion of its four wings. We are not aware of data on the vehicle’s terrestrial capabilities or performance results for either locomotion mode. The recently developed Microglider (Chap. 19) also locomotes both on the ground and in the air and implements a biologically inspired wing-folding mechanism. However, it hops into the air and then glides rather than being able to fly for extended periods as is the intended purpose of MALV and the Entomopter.

Nature has repeatedly demonstrated the need for multiple modes of locomotion, especially for small animals such as insects. Pure terrestrial locomotion may be impractical at this scale simply because of the distances that must be traveled to search for food, mates, etc. However, mono-modal aerial locomotion is also undesirable because it is impossible to stay airborne indefinitely, a variety of conditions (winds, etc.) make it difficult to land at exactly the desired location, and walking is far more energy efficient than flying for traveling short distances.

Utility for small robots often reflects the exact same problem domain as small animals; multiple modes of locomotion would represent a generational leap in their capability. Flight capacity could allow a vehicle to travel long distances and approach a general target area, while crawling locomotion would allow a range of additional possibilities (close inspection, surveillance, performance of tasks, etc.) unachievable by any vehicle existing today.

18.2 Biologically Inspired Structures for Flying and Walking

As stated earlier, abstracted biological inspiration focused on functionality of the MALV with technology presently available. Its mechanical design incorporated neuromechanical flight (deformable wing) and walking (compliant wheel-legs and axle joints) mechanisms, which were key to MALV’s locomotion capacity. The challenge was designing mechanisms for functionality in both modes while preserving as much mobility as possible in each individually.

18.2.1 Terrestrial Locomotion

The implementation of biological locomotion principles holds considerable promise for terrestrial locomotion. Legged animals exist and thrive at a wide range of sizes and are capable of overcoming obstacles that are on the order of their own size. Animal legs behave as if they have passive spring-like compliant elements when they are perturbed [6]. Alexander describes three uses for springs in legged locomotion, including energy absorption [4]. Jindrich and Full demonstrated this in an experiment wherein a cockroach was suddenly perturbed, too quickly for its nervous system to react [7]. It was shown that the passive compliance in its legs stabilized its body. Similar stability benefits are achieved through compliant elements in the legs of the RHex robot [10], which preceded WhegsTM.

Locomotion studies on cockroaches have elucidated several critical behaviors that endow the insect with its remarkable mobility [47]. During normal walking, the animal uses a tripod gait, where adjacent legs are 180° out of phase. The cockroach typically raises its front legs high in front of its body, allowing it to take smaller obstacles in stride, but when climbing larger obstacles, the animal moves adjacent legs into phase, thus increasing stability.

These benefits have been captured in design through the WhegsTM concept (Fig. 18.1), which served as the basis for the terrestrial locomotion of MALV. WhegsTM has spawned a line of robots that implement abstracted biological inspiration (based on the cockroach) for advanced mobility. Compliance is implemented into WhegsTM legs in two ways: radially for

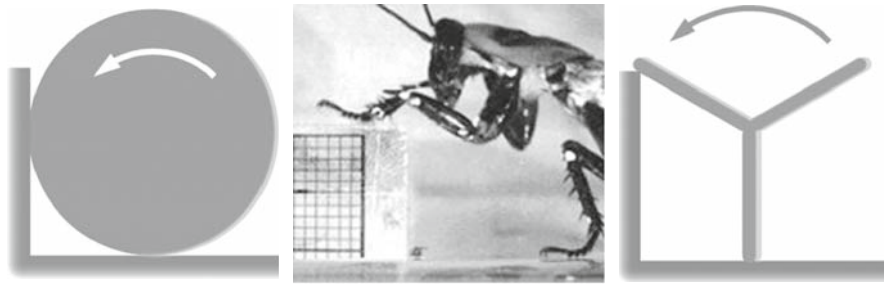


Fig. 18.1 The wheel-leg provides a compromise between the efficiency and ease of propulsion of a wheel and the terrain mobility of legs

shock absorption (one of the three uses of springs in legged locomotion cited by Alexander [4]) and torsionally for gait adaptation, leading to improved traction and stability [9]. Torsional compliance allows for a single motor to drive six three-spoke wheel-leg appendages in such a manner as to accomplish all of the locomotion principles discussed above. WhegsTM robots are also scalable, with successful robots being developed with body lengths ranging from 89 cm down to 9 cm.

This concept has been extended to Mini-WhegsTM (Fig. 18.2) that offer a combination of speed, mobility, durability, autonomy, and payload for terrestrial micro-robots. Mini-WhegsTM robots are extremely fast (10 body lengths per second) in comparison to most other legged robots and can climb obstacles taller than the top of their bodies [22]. The wheel-leg appendage

results in a natural “high stepping” behavior, allowing the robot to surmount relatively large obstacles. These vehicles have tumbled down concrete stairs and been dropped from heights of over 10 body lengths, without damage. Mini-WhegsTM have also carried over twice their body weight in payload [22].

18.2.2 Compliant Wings for Aerial Locomotion

A rigid leading edge, chord-wise compliant wing design is the basis for MALV’s aerial locomotion. The compliant wing inspired by flying animals has several advantages over similarly sized rigid-wing vehicles [1]. Delayed stall allows the vehicles to operate at slower speeds. Improved aerodynamic efficiency reduces the payload that must be dedicated to energy storage. Passive gust rejection significantly improves stability.

It has been well established that the aerodynamic efficiency of conventional (smooth, rigid) airfoils is significantly compromised in the Reynolds number (Re) range between 10^4 and 10^6 . This Re range corresponds to the class of craft referred to as micro-air vehicles [48]. In fact, the ratio of coefficient of lift (C_L) to coefficient of drag (C_D) drops by nearly 2 orders of magnitude through this range. With smooth, rigid wings in this Re range, the laminar flow that prevails is easily separated, creating large separation bubbles, especially at higher angles of attack [49]. Flow separation leads to sudden increases in drag and loss of efficiency. The effects of the relationship discussed above are very clear in nature. Consider, for example, the behaviors of birds of various sizes. Birds with large

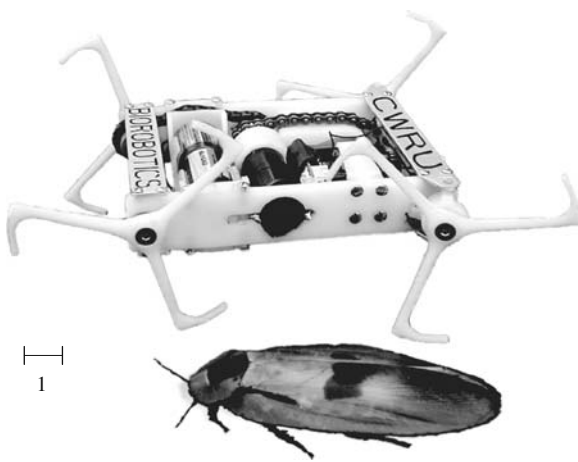


Fig. 18.2 Photograph depicting the relative sizes of a Mini-WhegsTM and a *Blaberus giganteus* cockroach. Scale is in centimeters (figure courtesy of Andrew Horchler)

wingspan, with a fixed wing $Re > 10^6$, tend to soar for prolonged periods of time. Medium-sized birds utilize a combination of flapping and gliding, while the smallest birds, with a fixed wing $Re < 10^4$, flap continuously and rapidly to stay aloft.

Other major obstacles exist for flight at this scale [1]. Earth's atmosphere naturally exhibits turbulence with velocities on the same scale as the flight speed of MAVs. This can result in significant variations in airspeed from one wing to the other, which in turn leads to unwanted rolling and erratic flight. The small mass moments of inertia of these aircraft also adversely affect their stability and control characteristics; even minor rolling or pitching moments can result in rapid movements that are difficult to counteract.

A rigid leading edge, chord-wise compliant wing addresses these issues for MALV's aerial locomotion capabilities. Through the mechanism of passive-adaptive washout, a chord-wise compliant wing (first implemented in the University of Florida (UF) [1]) overcomes many of the difficulties associated with flight on the micro-air vehicle scale. Adaptive washout is a behavior of the wing that involves the shape of the wing passively changing to adapt to variations in airflow. For example, an airborne vehicle may encounter a turbulent headwind, such that the airspeed over only the right wing is suddenly increased. The compliant wing structure responds to the instantaneous lift generated by the gust to deform in a manner similar to Fig. 18.3. This is referred to as passive-adaptive washout and results in a reduction in the apparent angle of attack and a subsequent decrease in lifting efficiency, as compared to the non-deforming wing. However, because the air velocity over the deformed wing is higher, it continues to develop a nearly equivalent

lifting force as the flat wing. Similarly, as the airflow over the wing stabilizes, the wing returns to its original shape. This behavior results in a vehicle that exhibits exceptionally smooth flight, even in gusty conditions; our own MALV flight tests have been conducted in the presence of winds that precluded the flight of larger (2+ m wingspan) rigid-wing aircraft. While quantification of this effect is difficult, feedback from highly skilled pilots has confirmed the efficacy of flexible wings in gusty environments.

18.3 MALV Design and Development

18.3.1 Methodology

18.3.1.1 Locomotion Mechanisms

The function of MALV is to carry a sensor payload, fly a long distance, and then land and move on the ground for a short distance, all while relaying sensor (e.g., visual) information to a remote location. For flight, a flexible wing was first selected over rigid or flapping wings to provide the best combination of controllability, payload capacity, speed, and efficiency (for long-distance missions) in the critical size range. Next, a range of terrestrial locomotion mechanisms were assessed for integration onto a MAV. One possibility was to attach free-spinning wheels to the fuselage of a MAV and use its propeller to drive the vehicle on the ground and in the air. Our experiments demonstrated that such a vehicle can land and takeoff from smooth firm terrain. However, this device had extremely poor ground mobility on rugged terrain. The propeller had a strong tendency to collide with obstacles, thus severely restricting ground mobility. Ground locomotion also suffered due to the fact that the forward thrust of the propeller was, out of necessity, above the wheel axle, creating a torque that pitched the vehicle forward. Therefore, when the wheels contacted an obstacle, the vehicle would often pitch forward nose first rather than actually moving forward. A possible alternative to this involved directly powering wheels attached to the fuselage, yet the vehicle's mobility would still be limited as it would not be able to climb obstacles even a small fraction of its own height. Legged locomotion mechanisms were judged to be too complicated, delicate,



Fig. 18.3 The chord-wise compliance of a flexible wing allows for passive-adaptive washout, increasing stability of the aircraft

and heavy at this time for use on a vehicle capable of both flight and crawling. We therefore chose to integrate flexible wing and wheel-leg (WhegsTM) locomotion mechanisms to design MALV.

18.3.1.2 Multi-modal Mobility Trade-Offs

A design analysis was performed to determine how to best integrate flight and ground mobility mechanisms. If a crawling robot was simply attached to the bottom of a MAV, the resulting vehicle would be too heavy to fly unless its wingspan were greatly increased. Therefore, a trade-off analysis was done to determine the most important parameters for ground locomotion and MAV locomotion. The successful MALV design preserves those parameters as much as possible. Less important design parameters were compromised to improve overall vehicle performance. In the case of a conflict where parameters important for flight were severely deleterious to ground mobility, a morphing mechanism was employed to resolve the problem. In the trade-off analysis flight was assumed to be the limiting condition because of energy demands and the larger payload enabled by crawling structures.

In flight, legs increase drag and reduce controllability. Furthermore, their associated mass reduces payload and can alter flight stability. On the ground, wings, propellers, and tails limit payload and impede mobility in confined spaces. The fuselage of an aerial vehicle tends to be long to increase its stability, but on the ground a long chassis causes the vehicle to high center on obstacles. On the ground, more legs can increase a vehicle's stability and mobility, but in the air they add drag and mass. These design inconsistencies broadly fell into two categories: mass and geometry.

Wheel-legs were judged vital to the ground mobility of MALV. However, their implementation was reconsidered to improve the overall performance of the vehicle. Past wheel-leg robots in small sizes typically had four wheel-legs driven by one propulsion motor and its front wheel-legs are steered. The front wheel-legs are most important because they reach in front of the vehicle and on top of obstacles in the vehicle's path to lift and pull the vehicle forward. WhegsTM are designed this way to model the front feet of cockroach, which lift high and in front of the animal to overcome obstacles [47]. To reduce mass and complexity, testing of the ground mobility of a MALV was executed with two

wheel-legs instead of four. The wheel-legs were placed in the front and to the side of the propeller. The rear of the fuselage dragged on the ground. We found that a MALV with this configuration could move forward over obstacles similar in height to a comparably sized Mini-WhegsTM robot. Additionally, the fuselage provided a tail-like action that prevented the robot from flipping onto its back, which happens when a purely terrestrial vehicle attempts to surmount obstacles very tall relative to its height. The drawback to this design is that MALV's mobility in reverse on rugged terrain was poor because the fuselage impacts irregularities and impedes motion. However, the weight savings justified the two-wheel-leg design.

Wheel-leg steering vs. differential steering was also contrasted in traded off design studies. Wheel-leg steering requires the wheel-legs to be placed further outboard on the wings so they do not strike the propeller when they are turned. Either design requires two motors. The differential steer design was chosen because no steering mechanism is required; the design is simpler and MALV can turn more sharply in this configuration.

Efficient hybrid designs can reduce mass by integrating structural, sensor, actuator, and power components. In MALV, the fuselage of the aircraft is also the chassis of the ground vehicle. Its shape has been changed to meet design criteria for flight and ground systems. MALV uses the same cameras in flight and ground locomotion to transmit video to a remote base. The same motor could be used for both flight and ground mobility in a manner akin to insects using large muscles to drive their body-coxa leg joints and flap their wings [50, 51]. However, this idea was abandoned for the first-generation robot because the complexity overrode possible mass reduction. A transmission would be needed because the wheel-legs must turn much more slowly than the propeller. The propeller shaft and wheel-leg axles are perpendicular, which also increase transmission complexity. Furthermore, a clutch would be needed to switch from propeller to wheel-leg drive. For these reasons we chose to use different motors for flight and ground mobility.

Wings provide a geometric inconsistency that cannot be compromised. Wings are clearly essential for flight, but are an impediment for ground locomotion especially when MALV is moving through narrow spaces. Birds and insects fold their wings when they are on the ground to eliminate impediments to motion.

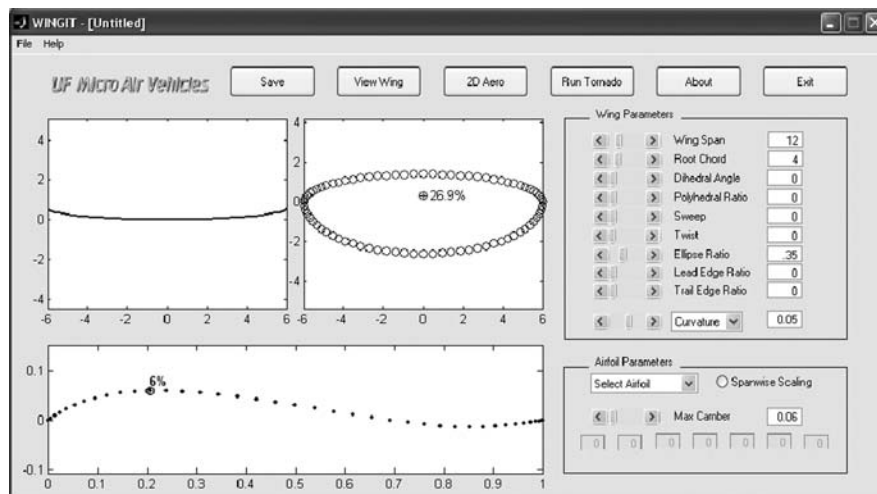


Fig. 18.4 User interface of the MAVLab design software

An insect-like wing-folding mechanism was therefore developed for MALV that mimics this action. It can stow its wings on its back when moving on the ground.

18.3.1.3 Design Summary

Simply attaching wheel-legs to a MAV was inadequate to design an efficient MALV. As is described above and in more detail in the following, a range of parameters were optimized for trade-off in the vehicle design space, compromised where necessary, and implemented following a system's approach focused on coupling between mechanisms for the design of each component. The resulting MALV achieves its goals of air and ground locomotion, but, because of necessary design trade-offs it is not yet as agile on the ground as Mini-WhegsTM and has less payload capacity and is less controllable than a flexible wing MAV.

18.3.2 MALV Design Implementation

Based upon weight estimates and initial flight testing, the lift capacity of a 30 cm wingspan MAV was determined to be sufficient to carry the additional weight associated with components needed for terrestrial locomotion.¹ Analysis of existing technology led to the

selection of R/C hobby servos as the power plants to drive the wheel-leg appendages. Modified R/C servos were chosen due to their light weight and ease of implementation. The modification allows for continuous servo rotation after which the integrated position control electronics act as speed controllers so that the servos can receive commands and power directly from the receiver. This process avoided the weight of additional speed controllers. Since one R/C servo was used for each wheel-leg, this configuration required a five-channel receiver (flight motor, elevator, rudder, left wheel-leg motor, and right wheel-leg motor), subsequently adding weight. The extra mass associated with the implementation of terrestrial walking was approximately 25 g, resulting in a 120 g projected mass.

Beginning with the estimated total vehicle mass of 120 g and the established maximum dimension of 30 cm, a new compliant wing was designed to provide the necessary flight characteristics for the vehicle. A software package (designed at the University of Florida) was used to identify an efficient wing shape, within the defined parameters, capable of producing the necessary lift. Efficiency (lift/drag) and coefficient of moment were also important constraints. Using the graphical user interface (GUI) (Fig. 18.4) all the critical wing parameters, including wingspan, root chord, sweep, ellipse ratio, and curvature, were selected for desired flight performance.

Real-time output from the GUI allows the designer to alter construction parameters until the desired characteristics are obtained. The program outputs 2-D aero-

¹ Initial performance specifications also called for a wingspan <33 cm for device portability.

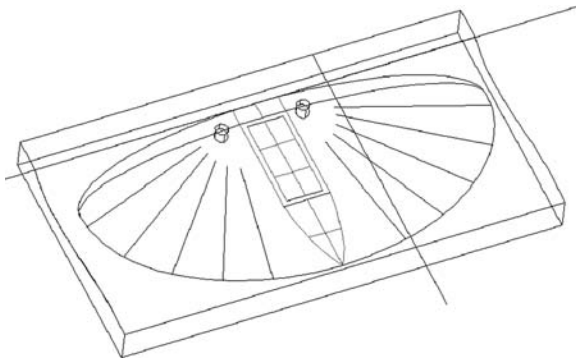


Fig. 18.5 A CAD solid model of the wing tool

dynamic parameters for the wing (coefficients of lift (C_L), drag (C_D), and moment (C_M), as well as C_D/C_L), key geometric features (planform area, aspect ratio, and location of aerodynamic center), and three views of the resulting wing. While MALV operates in an Re range where classical aerodynamic calculations break down, prior experience with the MAVLab software confirms the utility in using the software for initial airfoil design. Once satisfactory wing design parameters are identified an output script file is generated. This script file is then imported into a CAD program (Fig. 18.5), where it is converted into CNC tool paths for milling of a wing “tool.” The wing tool is a mold upon which the wing will be laid out during composite fabrication. The tool confers upon the wing the desired airfoil shape. The software automatically scales and translates the airfoil shape so that the entire leading edge of the wing lies in a horizontal plane.

After the wing tool is milled, it is prepared for the fabrication process [52]. First, a layer of release film is applied to the tool to prevent any resins or adhesives from bonding to and damaging the tool. A schematic of the wing layout (including the leading edge, battens, and canopy) is placed on the tool and a second layer of release film is applied. Using unidirectional and woven resin-impregnated (prepreg) carbon fiber, the wing structure is laid out on the tool. The wing fabric, a polycarbonate-coated polypropylene, was selected due to its compliant properties akin to a natural wing. The fabric is then overlaid onto the structure. Additional layers of carbon fiber were applied to form a skeleton for the wing akin to a flying animal’s wing. The carbon fiber skeleton maintained the general shape of the wing while still enabling the polypropylene to warp in flight for neuromechanical stability. The choice of a flexible wing design does introduce the potential for

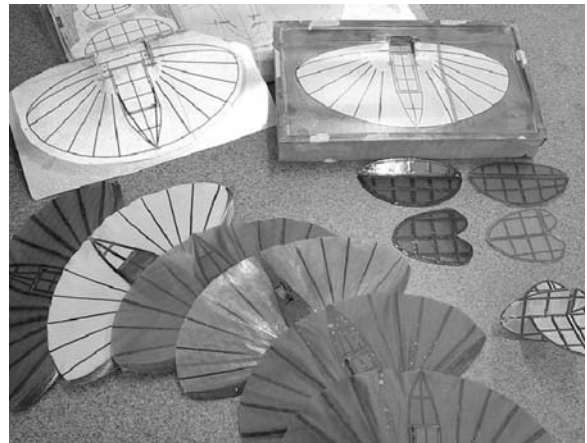


Fig. 18.6 Wing tools, tail sections, and a series of fabricated wings

aerodynamic dissimilarities between the wings on the opposite sides of the vehicle. However, experience has demonstrated that the flexible wing design is robust enough that a reasonable level of care during fabrication is sufficient to produce “equal” aerodynamic properties between the wings. “Reasonable care” includes controlling the tension applied to the wing fabric and maximizing the symmetry in the battens. Samples of wing tools with an array of completed wings and tail sections are pictured in Fig. 18.6. It should be noted that the compliant wing and skeletal structure may also enable MALV to fold its wings in an insect-like manner (Fig. 18.7).



Fig. 18.7 Three completed vehicles are shown with a series of fuselage tools and an array of investigated wing fabrics. The bottom right vehicle shows the wing-folding concept

In addition to wing selection, the fuselage had to be designed to integrate terrestrial walking. Three issues were of critical importance in MALV fuselage design: (1) physical incorporation of the wheel-leg drive motors within the fuselage, for durability; (2) maintaining the desired horizontal position of the center of gravity (CG) for flight and land mobility; and (3) locating the wheel-legs forward such that their feet contact obstacles before any other parts of the vehicle for obstacle climbing. The wing analysis described above identified the theoretical location of the wing aerodynamic center (AC). Pitch stability of an aerial vehicle is maintained by locating the CG forward of the AC. If the downforce generated by the tail section is too large, the vehicle pitches up, resulting in a more positive angle of attack for both the wing and the elevator. The changes in lift from the two surfaces counteract the original discrepancy between the desired and actual moment balance on the vehicle. Fortunately, the second and third considerations are complementary because placing the wheel-legs forward on the fuselage also moved the CG forward.

After assembling a list of the components and their masses, the fuselage length was determined that would accommodate placement of the CG in the desired horizontal location with the wheel-legs in front of the vehicle. The fuselage was widened for the wheel-leg drive motors. Fuselage tools and an array of wing fabrics and completed MALV vehicles are also depicted in Fig. 18.7.

To take full advantage of the strength and weight of the carbon composite material, tools were fabricated to integrate the servomotor output horn into the wheel-leg (Fig. 18.8). The carbon fiber also serves to rein-

force the nylon servo horn in this configuration. The tool allows for endowing the wheel-leg spokes with the necessary “splayed” shape. This shape allows the wheel-legs to reach out around (and in front of) the propeller (vehicle in lower right corner of Fig. 18.7), while minimizing the necessary width of the fuselage.

In addition to enabling mobility, compliant structures in biological organisms also help to reduce damage to mechanical elements during impact, as one of the three uses of springs in legged locomotion as described by Alexander [4]. This is of critical importance to MALV to maintain the functionality of the vehicle during the impact of landing. Multiple wheel-leg designs for MALV were evaluated with this in mind against two criteria: (1) surviving the landing process and (2) facilitating terrestrial locomotion. During landing, a large torsional impact load is placed on the entire system, in particular terrestrial locomotion components including the wheel-legs and the drive motors. A range of possible solutions to this problem were considered including developing a small slip clutch mechanism to allow the wheel-leg appendages to “freewheel,” designing a compliant mechanism within the wheel-leg joint, and designing a new compliant wheel-leg “foot” that would insulate the drive motor from landing impact. Explicit research was initiated to explore muscle-like joint and actuator compliance akin to structures found in nature. Traditionally, robot design has striven to maximize the impedance between actuator and load and to minimize joint compliance, given that compliance can introduce uncontrollable and underactuated degrees of freedom. For MALV, advantages of leg or joint compliance ideally will lead to (1) lower inertial forces with compliant joints, (2) lower reflected impedance with drive motors, (3) potential for energy storage and restitution, (4) passive dynamical compensation for destabilizing effects resulting from transmission lag, (5) greater shock tolerance and reduced damage due to the neuromechanical properties of compliant/elastic elements (most important for landing and crawling in sequence), and (6) conforming to the terrain for improved traction. Uses (3) and (5) were cited by Alexander as used by animals in legged locomotion and (6) is a further use that MALV has in common with these animals.

It was found that compliant wheel-legs and axles lent dynamic mechanical properties enabling these advantages. Testing demonstrated these to be the most durable, most likely to survive landing impact, and best

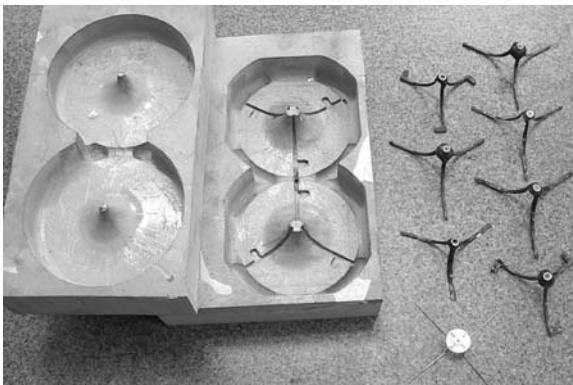


Fig. 18.8 Two wheel-leg tools and several tested designs



Fig. 18.9 MALV II has piano wire wheel-legs that are compliant on landing and resist becoming embedded in the substrate. These wheel-legs also enable it to crawl through grassy areas and climb obstacles taller than its leg length

protected the system (drive motors, etc.) by providing neuromechanical rejection of high-frequency, high-impact disturbances. The simplest design implemented was a four-spoke wheel-leg fabricated from spring-tempered stainless steel wire (shown at the bottom of Fig. 18.8). A wire diameter of 1.19 mm (0.047 in.) provided sufficient compliance to absorb the landing impact, but not buckle undesirably during terrestrial locomotion. However, the lack of proper feet (sharp spokes in this wheel-leg design) caused a tendency to become lodged in both soft and obstacle-rich terrains. An improved design utilizing the compliance of the spring steel, implementing an efficient foot shape (identified in previous crawling research [53]) and incorporating joint compliance in the axle provided much improved performance. Figure 18.9 shows the resulting wheel-leg. The closed-loop foot avoids difficulties associated with sharp spokes becoming stuck in the substrate, compliance in the steel and leg shape increases mobility, and compliance in the axle and leg insulates the terrestrial crawling system from damage on harsh impact.

Figure 18.10 shows the utility of the closed foot and compliance in the wheel-legs of the MALV in a

crawling sequence as it maneuvers over uncertain terrain, including a shifting rubble surface and ground obstacles nearly as tall as the vehicle. A comparably sized wheeled or tracked vehicle would have difficulty climbing or maintaining stability on this shifting terrain.

18.3.3 Wing-Folding Mechanisms

18.3.3.1 Introduction

Because some design parameters cannot be compromised in a trade-off analysis, we enhanced MALV's mobility by morphing its physical geometry to suit its active mode of locomotion. For example, a particular wingspan is necessary to create the desired lift for aerial locomotion, but that wingspan is an impediment to ground locomotion when MALV is moving through narrow spaces.

Our initial MALV designs utilized a wing that was constantly deployed during both terrestrial and aerial locomotion. This reduced the vehicle's ground

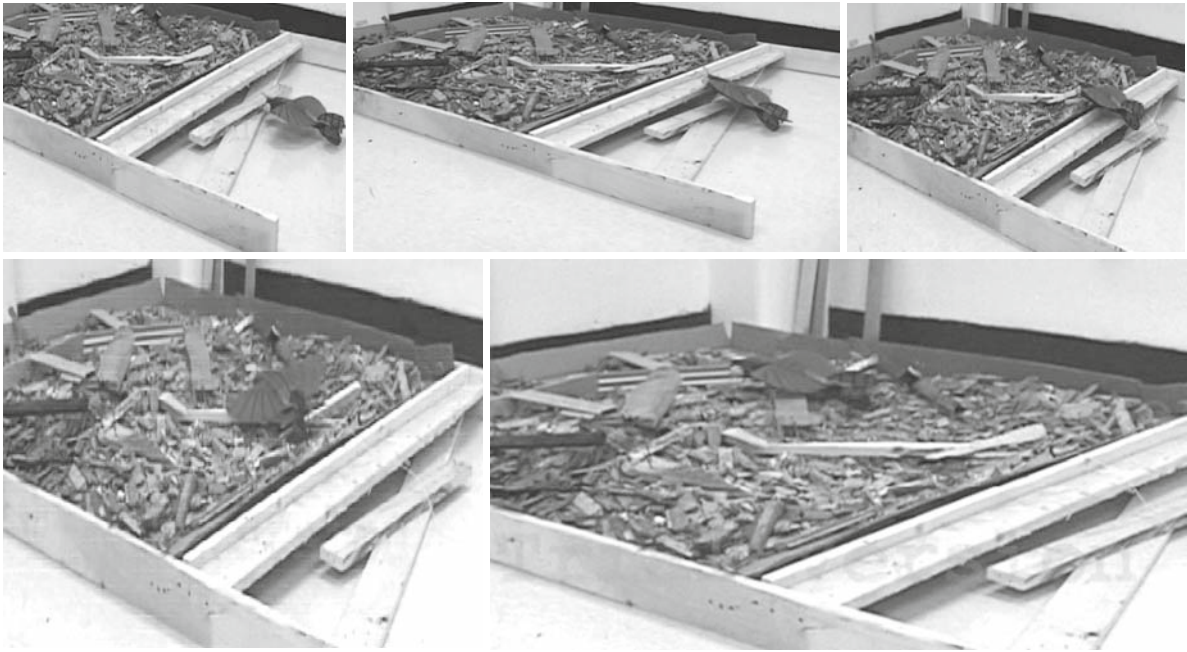


Fig. 18.10 MALV II Demonstrating climbing and arduous terrain navigation over terrain akin to rubble encountered in disaster relief operations

maneuverability in confined spaces, unnecessarily exposed the wings to damage from the environment, and made the vehicle difficult to pack for transport when not in use. Insects, bats, and birds address this

issue by retracting their wings against their body. We designed similar mechanisms for MALV, as shown in Fig. 18.11 where the robot folds its wings before walking through a narrow opening.



Fig. 18.11 MALV is unable to pass through a small space with its wings deployed. By folding its wings back, it is able to reduce its physical size, allowing it to pass through the space

18.3.3.2 Mechanism Design

To successfully design a wing-folding system, two different areas must be addressed: the folding mechanism itself and the design of the folding wing. Each of these poses unique challenges. The folding mechanism must be able to passively sustain in-flight forces, produce sufficient force to tension the fabric wings, provide the necessary range of motion, and be lightweight. The folding wings must be able to provide repeatable folding behavior with a flexible skin, resist drooping caused by gravity and upward bending due to lift, and be able to fold in a compact manner without impairing the vehicle's ground mobility.

The folding mechanism uses a four-bar linkage actuated by a servo and a transmission link. The linkage employs a retractable landing gear mechanism shown in Fig. 18.12. For MALV, the landing gears are modified with an aluminum arm that allows more torque to be transmitted to the system. The implementation of the folding mechanism is shown in Fig. 18.13.

In operation, the servo arm pushes the transmission rod, which deploys or retracts the landing gear. The gear rotates the rigid leading edge of the wing which causes the entire wing to either deploy or retract. The

landing gears have a 90° range of motion by themselves, so the motion of the wing is limited by its structure and the angle through which the servo is able to move the landing gear.

The folding wing design was implemented using a carbon fiber enclosure to permit wing rotation and also provide bending stiffness. An illustration of the carbon fiber enclosure is illustrated in Fig. 18.14. The top and bottom enclosures allow the leading edge of the wing to rotate and the window in the canopy gives the retract mechanism a free path of rotation. These enclosures in combination with struts and crossbars stiffen the wing in vertical bending. Experimental studies were conducted to determine a batten configuration that provides the necessary wing stiffness while still allowing for wing folding. Three different batten configurations are shown in Fig. 18.15.

The battens emanate from the axis of rotation of the wing to allow folding. Batten designs 1 and 2 were found to hinder wing folding because they added too much stiffness at the junction between the canopy and the leading edge. When the wing is folded back, the fabric deflects the most at this point, so adding stiffness to this area prevents the fabric from deforming. Batten design 3 adds stiffness to the wing without adding stiffness to this particular area. This allows the

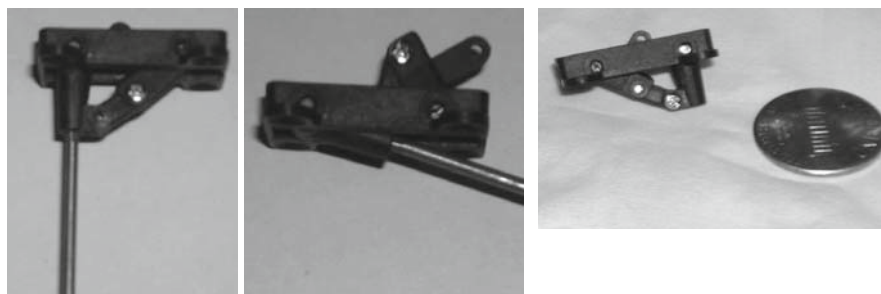


Fig. 18.12 GWS pico retractable landing gear, deployed (*left*) and retracted (*center*) and compared for size with a U.S. penny (*right*)

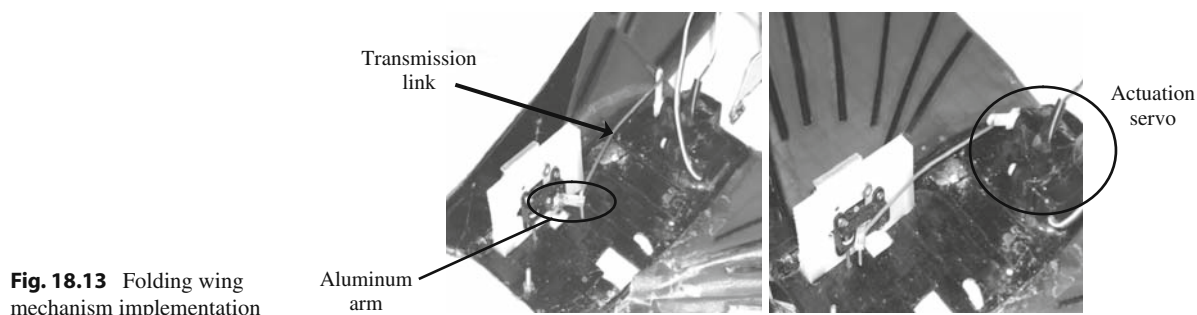


Fig. 18.13 Folding wing mechanism implementation

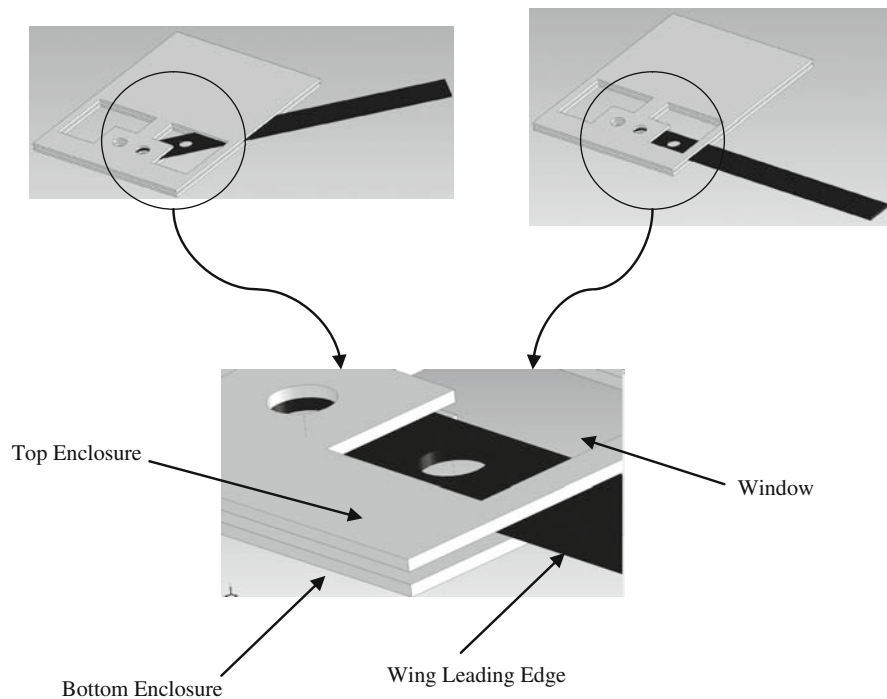
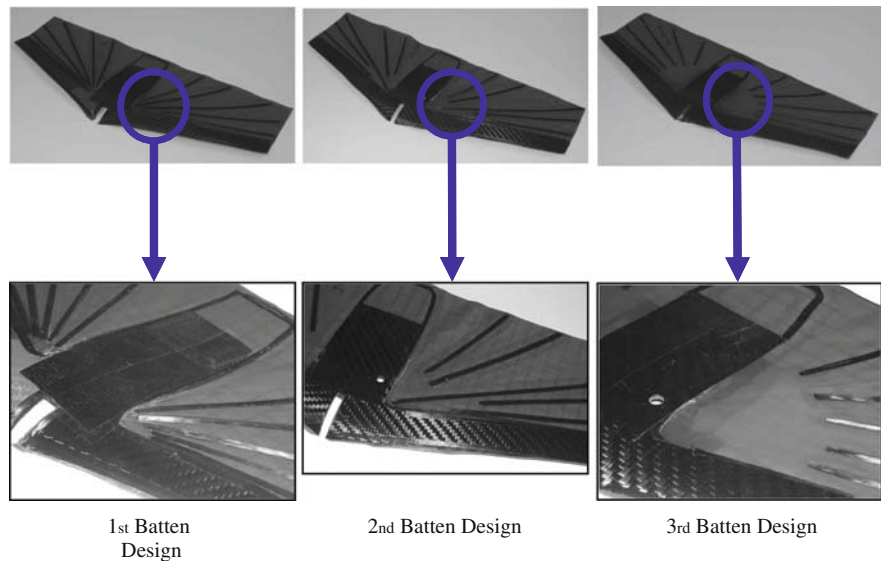


Fig. 18.14 Illustration of the enclosure concept. The enclosure is made from the center part of the wing that lies over the fuselage (canopy)

Fig. 18.15 Three different batten designs. Batten designs 1 and 2 hinder wing folding while batten design 3 allows rotation



fabric to deform as necessary. The final wing-folding system uses a modified version of the third batten design above (modified version shown in Fig. 18.16). When folded the width of the vehicle is reduced by a

factor of 2 (Fig. 18.16b). This wing-folding system is placed entirely on the wing, which allows a set of folding wings to be constructed independently from the rest of the aircraft.

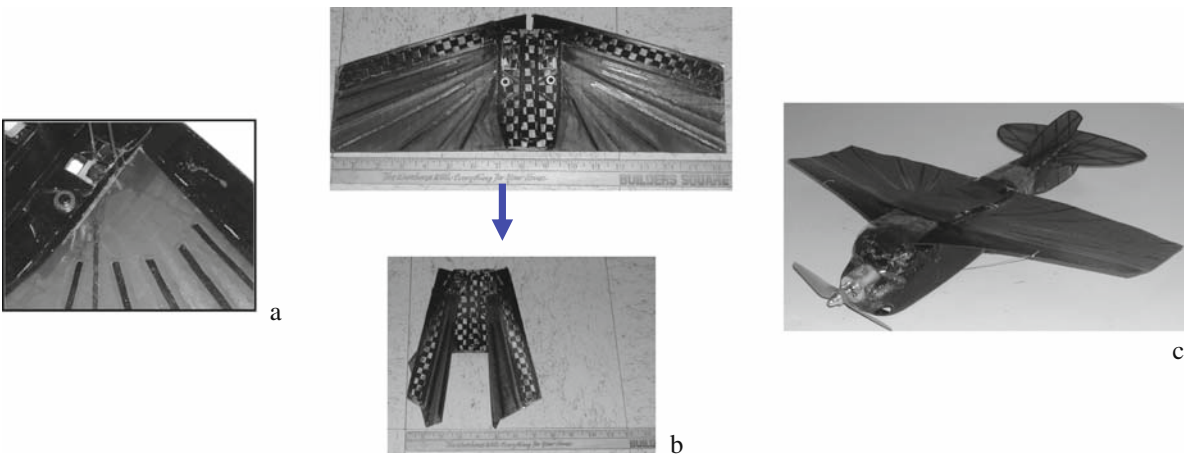


Fig. 18.16 (a) Batten design that allows for compact folding. (b) The wing is able to halve its size. (c) Morphing micro-air and land vehicle (MMALV)

18.4 Results and Performance Testing

18.4.1 Vehicle Description

Several iterations of the design and fabrication process led to the completion of a range of vehicles capable of aerial and terrestrial locomotion. The first vehicle had a solid carbon fiber wing which was built principally for testing the integration of wheel-legs with basic flying mechanisms. While significantly limiting the flexibility of the wing surface, this arrangement did allow for the implementation of aileron control, which provides more responsive control than the rudder/elevator system implemented on the second-generation vehicle (MALV II). However, the increased passive stability from incorporating the bio-inspired chord-wise compliant wing led to the adoption of MALV II as the standard vehicle. Table 18.1 lists the physical characteristics of MALV II.

The design process was predicated on the knowledge of the masses of the components that would be included in the vehicle. Drawing upon considerable

Table 18.1 Physical characteristics of MALV II. The location of the CG and the location of the wing leading edge are along the longitudinal axis, measured from the tip of the fuselage

Parameter	Value
Overall length	30.5 cm
Weight	118 g
Fuselage length	21.6 cm
Fuselage width	5.1 cm
Location of CG from fuselage tip	9.5 cm
Location of leading edge	6.9 cm
Leg length	4.2 cm
Track (distance between wheel-legs)	16.7 cm

experience in the design and testing of MAVs and terrestrial robots, components were selected (Table 18.2). Weight was the primary selection criteria among components that could provide the necessary thrust, control, sensing, and terrestrial power to perform the desired tasks.

Iterations on the MAVLab software generated the wing with the highest efficiency (C_L/C_D), within the prescribed dimensions that could generate the required

Table 18.2 List of critical components

Component	Specifications
Aerial propulsion motor	Feigao brushless DC motor ϕ 13 mm, 36 turn windings
Electronic speed controller	Castle Creations Phoenix 10 Sensorless ESC
Propeller	GWS EP3030 ($\phi = 76$ mm)
Control surface servos	Saturn S44 Digital Servo
Terrestrial drive motors	Maxx Products MX-50HP
Power storage	Polyquest 11.1 V, 600 mA h lithium-polymer battery

Table 18.3 Main wing data

Parameter	Value
Wingspan (b)	30.5 cm
Wing area (S)	364.4 cm ²
Wing loading	31.7 N/m ²
Aspect ratio (AR)	2.55

lift at 9 m/s airspeed. This value is derived from prior experience piloting flexible wing MAVs. Beyond this speed, the vehicle becomes more difficult to pilot. Wing parameters are listed in Table 18.3.

The wing planform is bounded by semi-ellipses at the leading and trailing edges. The root chord length of the wing is 15 cm, with the maximum width occurring 4.75 cm from the leading edge. The wing was mounted to the fuselage with an incidence angle of 8°, with respect to the thrust line of the motor.

Control surface parameters are shown in Table 18.4. The horizontal stabilizer was mounted parallel to the motor thrust line. The horizontal stabilizer/rudder unit comprises two half ellipses, with a major axis of 14 cm and minor axes of 4.763 and 2.223 cm, respectively. Approximately 2.58 cm² of the vertical stabilizer is occluded by the fuselage. By locating the rudder below the center of gravity (CG) of the craft, rudder deflection produces a sympathetic roll, i.e., a roll motion in the direction of the desired turn.

Table 18.4 Control surface data

Element	Area
Horizontal stabilizer	52.3 cm ²
Elevator	24.4 cm ²
Vertical stabilizer	52.9 cm ²
Rudder	5.0 cm ²

18.4.2 Multi-mode Locomotion

Table 18.5 summarizes the aerial and terrestrial locomotion characteristics of MALV II. The maximum flight time was determined experimentally (flying the plane until the battery could not produce necessary thrust). Maximum crawling time was estimated by experimentally determining the current draw for locomotion on flat terrain and comparing this to the battery capacity. However, its ground mobility is not restricted

Table 18.5 Nominal performance characteristics of the micro-air-land vehicle (MALV) II

Parameter	Value
Cruising air speed	11 m/s
Reynolds number	$\sim 1 \times 10^5$
Maximum flight time	15 min
Range (round trip)	4.9 km
Maximum terrestrial speed	0.33 m/s
Maximum crawling time	100 min
Range (round trip)	0.99 km

to flat terrain. It can crawl over grassy areas and climb obstacles higher than its leg length (Figs. 18.9 and 18.10). Both tests were performed with all video system components (see Table 18.7) onboard. Round trip range was calculated from the cruising speed and maximum flight time.

It is apparent from the table that MALV possesses strong aerial range for its size and is capable of considerable terrestrial locomotion within the capacity of a single battery pack. All control of MALV II is executed using standard R/C equipment. The transmitter's programmability facilitates fluid transition from flight to crawling control. During flight, the right joystick controls elevator (up/down, channel 1) and rudder (left/right, channel 2). Once the vehicle is landed, the operator switches the controller into ground mode, which then "mixes" the right joystick commands and transmits the results on channels 4 and 5. "Forward" (joystick up) sends positive signals to both channels, while "right" sends a positive signal to the left wheel-leg and a negative signal to the right wheel-leg for differential steering. "Backward" and "left" act conversely. Channels 1 and 2 are turned off during ground mode.

18.4.3 Transition Between Flight and Crawling

Beyond the capacity to both fly and crawl, perhaps the most challenging aspect of MALV design was to enable effective transition between the two locomotion modalities. MALV II is presently capable of transitioning from flying to crawling locomotion and, in some circumstances, capable of attaining flight from a crawling mode.

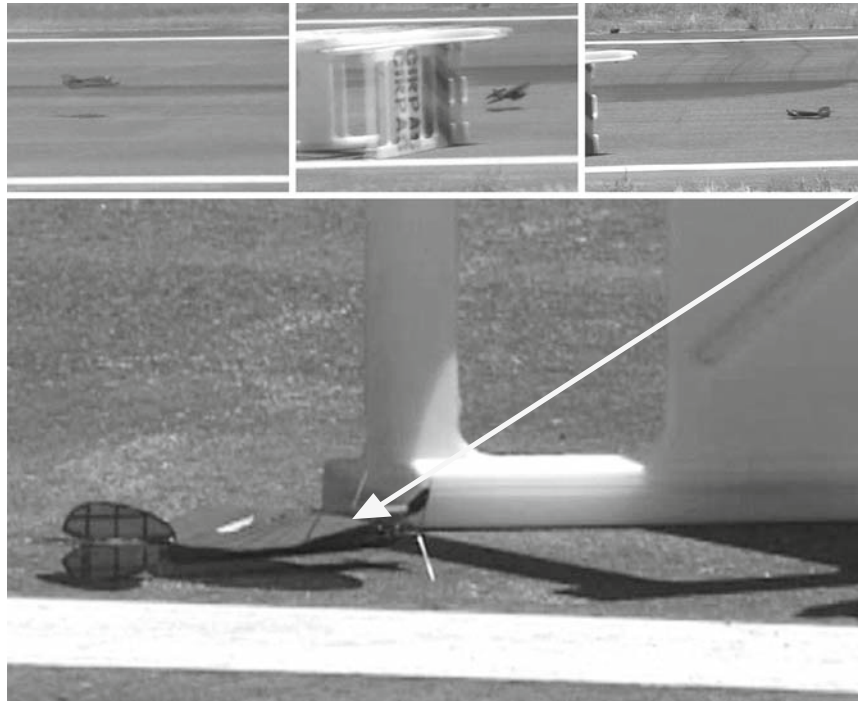


Fig. 18.17 Snapshots of MALV II transitioning from flight to crawling locomotion

18.4.3.1 Air-to-Land Transition

Figure 18.17 shows a snapshot sequence taken from a video of MALV flying, landing, and subsequently crawling (in this case to search for an object hidden in a road construction barrier). The dynamic mechanical properties of the vehicle absorb the energy of landing impact and enable effective and immediate crawling locomotion.

18.4.3.2 Land-to-Air Transition

The vehicle's ability to perform sufficiently at high angle of attack and low airspeed conditions resulted in a repeatable, successful takeoff capability from atop building structures two stories or taller. After the vehicle walks off the roof of the structure, it enters a powered dive, pulled down by both gravity and the propeller. As airspeed builds, the necessary lift is generated to arrest the fall and transition to flight phase. Takeoff from a sloped roof-top produces more consistent results than from a cantilevered plate. The vehicle is able to attain a higher ground speed on the declined

runway, thereby maintaining more favorable vehicle orientation at liftoff and gaining consistent separation from the building. Figure 18.18 shows this sequence. MALV has also been shown to take off from the ground on hard, smooth surfaces such as concrete and asphalt using its propeller thrust. The wheel-legs act like skids as the vehicle accelerates to takeoff speed in 3–5 m.

18.4.4 Sensor Capability and Integration

MALV II originally used a 7.4 V, 600 mA h lithium-polymer (Li-Po) battery. With this power source, its Feigao propeller motor was able to produce a cruising speed of 8 m/s (17.9 mph). The lift generated at this airspeed was nearly consumed by the weight of the terrestrial drive system and one camera/transmitter unit. Installing an 11.1 V, 600 mA h battery increased the cruising speed to 11 m/s. The increased lift supported the increased battery mass (59 g vs. 41 g), a second camera, an electronic switch to control camera signal transmission, and the added mass of a six-channel receiver. The camera transmitter operates in

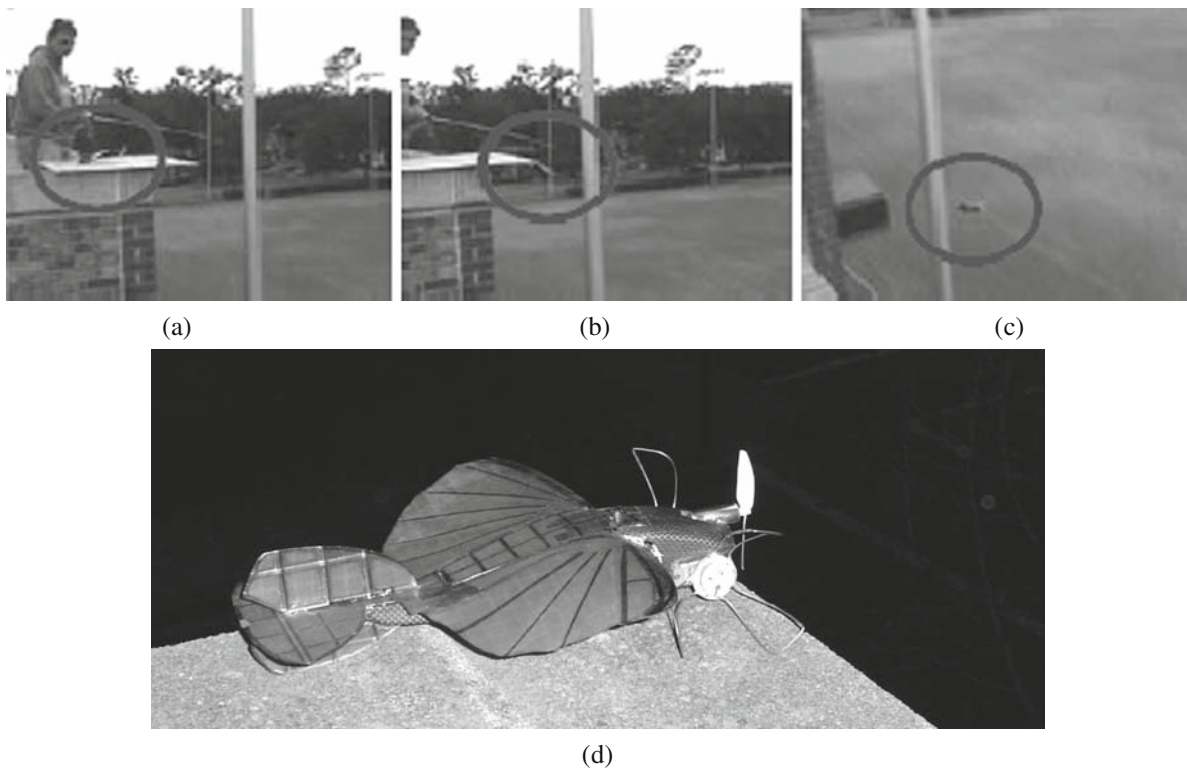


Fig. 18.18 (a) MALV nears the edge of the structure; (b) MALV walks off the building, entering a “power dive”; (c) lift is produced, and the vehicle pulls out of the dive; and (d) closeup of MALV prepared to walk off a building

the 2.4 GHz range. Figure 18.23 shows an image capture of the transmission during a normal flight. Future work is envisaged for vision-based vehicle navigation based on the camera feedback.

18.4.5 Flight Autonomy and (Video) Telemetry

Micro-aerial vehicles are very sensitive to disturbances such as wind gusts and deflections of the control surfaces, and therefore require considerable practice and talent to operate efficiently. Even if an operator were proficient at flying MALV via radio control, many situations can be envisioned that would prohibit this sort of continual monitoring. The urgency of relocation in no way diminishes the importance of the MALV task domain and clearly should not jeopardize that mission. Therefore, an autonomous control system and a remote sensor telemetry system are both critical to facilitate the eventual field utility of MALV.

An autonomous control system has been designed and implemented on the MALV for aerial waypoint navigation and a telemetry unit has been integrated onboard the plane capable of sending video feedback from the robot in both aerial and terrestrial modes of operation. This was accomplished through the integration of the Procerus Kestrel [54] autopilot, along with a modem, GPS receiver, telemetry antenna, and pitot tube into the MALV airframe. Table 18.6 details the

Table 18.6 Dimensions and weights of the MALV autopilot components

Item	Length (mm)	Width (mm)	Height (mm)	Weight (g)
Procerus autopilot	50.8	34.8	11.94	16.65
Aerocomm modem	41.91	48.26	5.08	21
Telemetry antenna	N/A	N/A	N/A	≤5
GPS receiver	21	21	9.6	12.6
Pitot tube	152.4	1.59	1.59	7
Total				62.25

Table 18.7 Dimensions and weights of the MALV video components

Item	Length (mm)	Width (mm)	Height (mm)	Weight (g)
600 mW video transmitter	49.53	24.13	8.13	14
Two color video cameras (air and ground views)	8	8	9.5	3 ($\times 2$)
Video antenna	N/A	N/A	N/A	< 5
5-V voltage regulator	40	15	4	6
11.1 V, 1500 mA h battery	79	40.64	18.04	113
Total				144

components of the autopiloting and telemetry system for the MALV, their dimensions, and their weight.

In order to ensure video feedback from the plane to an operator, a video telemetry system was also implemented on the MALV. The video feedback system requires a video transmitter, a video camera, an antenna, and a voltage regulator to direct power from the MALV battery. A summary of the video system and power source components is provided in Table 18.7. Note that two cameras were integrated onto the vehicle: one directed downward for aerial surveillance and one directed upward for terrestrial. This was judged to be simpler than one servo-mounted camera, although future work will explore this capacity.

The video system and power source component selection resulted in an estimated addition of nearly 210 g to the aircraft's gross takeoff weight (GTOW); the total weight of MALV II was 90 g without wheel-legs and 116 g with wheel-legs. Although we expect future versions of these components to be significantly smaller and lighter, we initiated a new MALV design to test the capacity of our design with this additional

payload. Design modifications included increasing the wingspan of the MALV as well as the size of the motor that propelled the system. The intent was to increase the wingspan only as much as necessary in order to provide the requisite lift. These efforts resulted in an aircraft that measured 39 cm long and with a wingspan of 41 cm. This new version, MALV III, was given a substantially larger fuselage to accommodate the addition of the above-listed components. When the new airframe was built and before the additional components were installed, MALV III without the wheel-leg drive system weighed 130 g, only 12 g more than the 30 cm model. Both versions of the MALV are shown in Fig. 18.19 (left) along with open view (right) of MALV III illustrating component integration.

18.4.5.1 Autopilot Tuning

The biologically inspired mechanisms in MALV facilitated smooth integration of the vehicle control system. Passive compliance in both the wings and wheel-legs eliminated the need for high-frequency feedback controllers adjusting to aerial disturbances and varying terrestrial terrain, thus allowing for simpler linear control. The autopilot control system therefore consisted of PID control loops regulating roll, pitch, yaw, and airspeed which were tuned to direct heading toward GPS waypoints. Control inputs were to the propeller motor and servos directing control surface deflections to the elevator and rudder. All information from the plane was transmitted to a ground computer with a digital map of the region of interest. New GPS waypoints were sent to the plane through the modem as

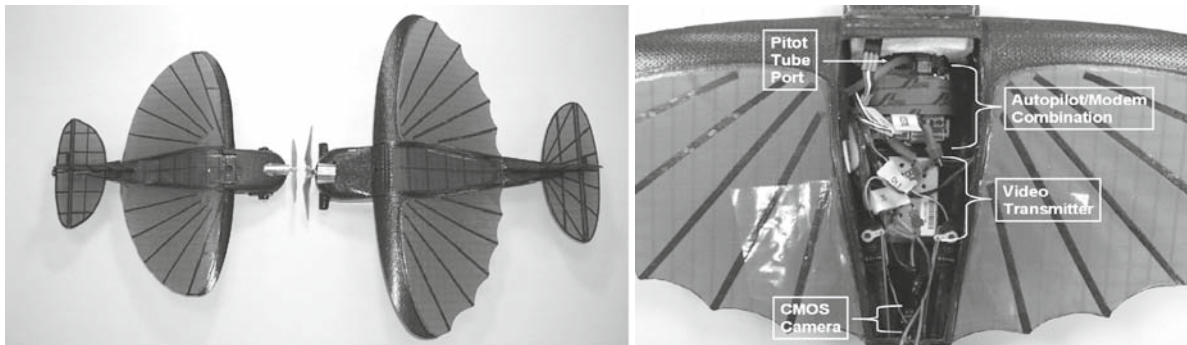


Fig. 18.19 The 30 cm and 41 cm wingspan versions of the MALV (left) and component integration for autopilot and video telemetry systems (right)

selected by a ground operator from the digital map. The gains for the control loops were found experimentally based on a series of test flights. This procedure was derived from that outlined in [54]. In ground mode, the operator would control the aircraft directly by giving combined or differential input to the wheel-leg motors since this requires no training or expertise whatsoever.

18.4.5.2 Results

Figure 18.20 delineates a typical MALV III experiment with six waypoints and the vehicle path highlighted. The waypoints were established with no less than 350 m in between them. Also shown are the takeoff (T), landing (L), and approach (A) points for the vehicle during the flight. Note that live video feedback from the plane was provided throughout the entire flight and in subsequent crawling locomotion. A waypoint was considered successfully reached if the vehicle was within 30 m during flight.

Figure 18.21 shows a series of timed snapshots of an unpiloted takeoff sequence where the MALV was tossed by an operator and autonomously begins waypoint navigation. In this experiment, MALV took approximately 4 s to reach a desired altitude of 100 m where its first waypoint was specified.

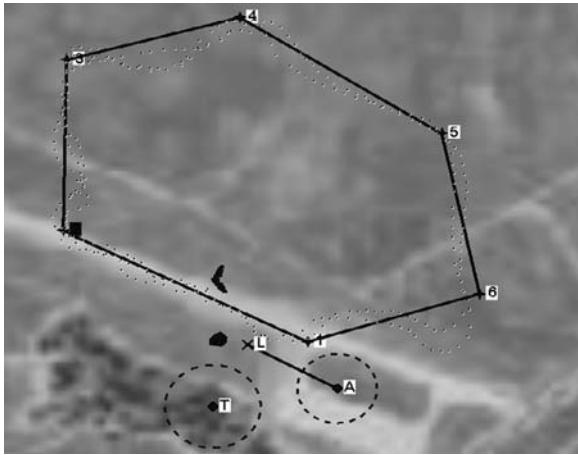


Fig. 18.20 Typical flight for MALV III performing waypoint navigation from waypoints on a digital map. The flight consisted of reaching each waypoint in numerical order. The *solid line* indicates the desired path and the *dotted line* shows two experimental flight paths. Takeoff (T), landing (L), and approach (A) points are indicated in the figure

As a part of evaluating the vehicle control system, the aircraft’s ability to hold both altitude and airspeed was also assessed. Table 18.8 enumerates these results over several flights with MALV III to reach waypoints while maintaining a certain commanded altitude and airspeed. The accuracy of the vehicle in holding desired altitude and airspeed was judged adequate for the surveillance tasks in this experiment and will be used as a basis for future mission planning. Note that the speed of the aircraft is slightly higher than MALV II given the larger motor powering the airframe.

A series of experiments were also executed to assess the quality and limits of the video telemetry system. Figure 18.22 shows snapshots of video transmitted by MALV III from an experiment where it was tasked to scout an area to locate a vehicle from the air, land near that vehicle, and crawl under it to inspect its undercarriage for any foreign objects. As mentioned earlier, MALV III was equipped with two cameras, one facing downward for aerial use and one facing upward for terrestrial use. The operator was given the option of switching between views of each camera depending on the locomotion mode of the vehicle. Experimental results in telemetry demonstrated the capacity of the vehicle to be commanded through the autopilot from more than 1.5 km and transmit video over distances greater than 0.5 km.

18.5 Conclusions

This chapter introduces a unique small (~30 cm maximum dimension) micro-air-land vehicle (MALV) drawing from locomotion principles found in legged and winged animals. Much of the success of MALV is due to two biologically inspired mechanisms integrated into its design: a compliant wheel-leg terrestrial running gear and chord-wise compliant wings. Its wheel-legs mimic leg motions while rotating continuously and enable it to climb over terrestrial obstacles that are taller than its legs. MALV survives hard landings on concrete because its flexible wheel-legs

Table 18.8 MMALV altitude and airspeed

Commanded airspeed	Range of airspeed held	Commanded altitude	Range of altitude held
14 m/s	10.5–16 m/s	66 m	50–84 m

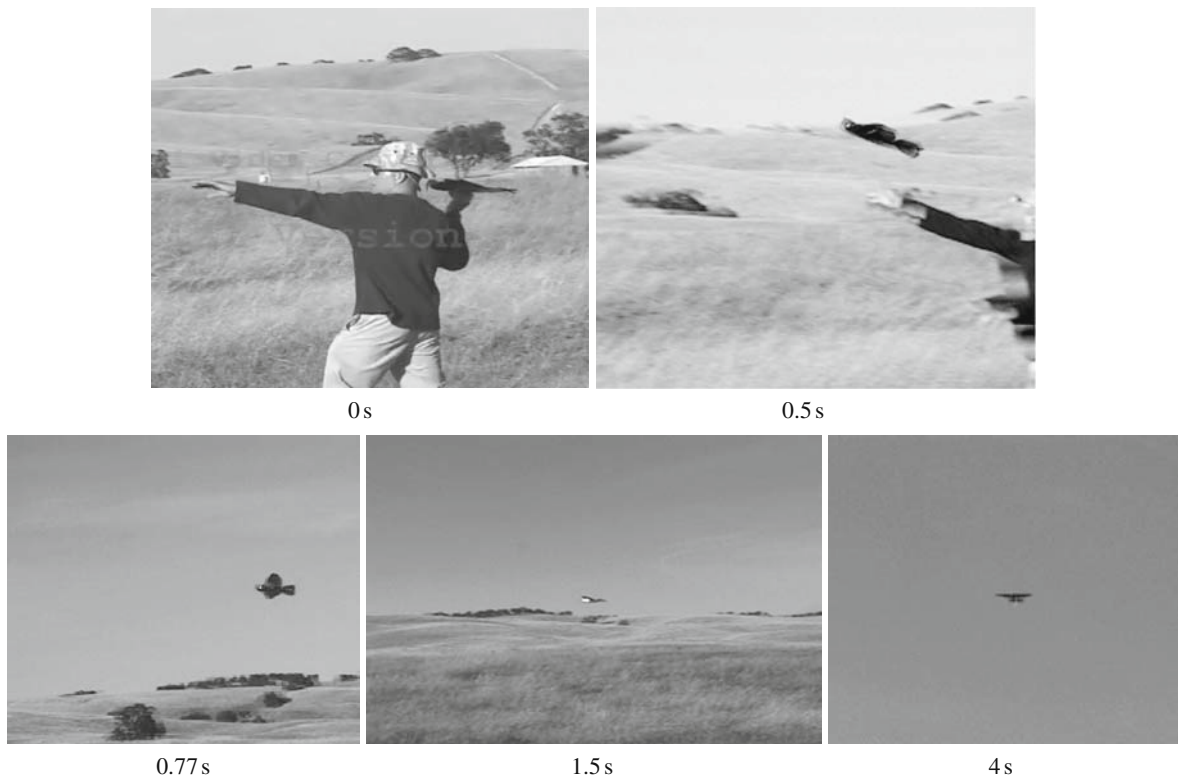


Fig. 18.21 Snapshots from MALV unpiloted takeoff. The operator gently tosses the vehicle and the autopilot brings it to its desired altitude of 100 m to initiate waypoint navigation



Fig. 18.22 Aerial video feedback from MALV III locating a vehicle from the air (*left*), MALV III crawling under the vehicle (*center*), and terrestrial video from MALV III locating a foreign object in the vehicle's undercarriage (*right*)

passively comply during impact reducing the magnitude of the force transmitted to its onboard components. This mimics the function of passive compliance found in the legs of an animal when it is suddenly perturbed. Likewise, MALV's chord-wise compliant wing overcomes many of the stability difficulties associated with flight on the micro-air vehicle scale through a mechanism observed in animal flight, passive-adaptive

washout, wherein the shape of the wing passively adapts to variations in airflow. The MALV is human portable, hand launched, and radio controlled. It can fly several kilometers, land, and then crawl for many meters around the landing site while surmounting tall obstacles relative to its height. MALV transmits back to the pilot video signals from its position in the air or on the ground. When it lands on a building or other

Fig. 18.23 Roads and cars are clearly visible in this image captured from a video transmitted from MALV II in flight



location that is at least two stories high, it can walk off the structure and retake to the air. Furthermore, it can takeoff from the ground on hard, smooth surfaces.

A slightly larger version of the vehicle, MALV III (41 cm maximum dimension), has also been developed that is capable of autonomous operation. The biologically inspired mechanism in MALV III enables smooth integration between the mechanics and control system, thus simplifying controller design. This vehicle can navigate aerial waypoints, accept commands from a user while in flight, and transmit video to a user in both aerial and terrestrial modes of operation. It should be noted that the slightly increased size of MALV III will most likely not be necessary for future operations given the rate of improvement in available micro-controllers, accelerometers, integrated autopiloting systems, and video telemetry. The components integrated on MALV III, for example, have very significantly decreased in size and weight in the last few years alone, and smaller versions have already become available from the time of the flight experiments to the time of this writing. The video transmission system has already been implemented onto the smaller MALV II airframe. Figure 18.23 shows a snapshot in flight from MALV II. Future designs are envisaged based on its 30 cm wingspan, with smaller versions already under development.

To our knowledge MALV is the first successful vehicle at this small scale to be capable of both powered flight and terrestrial locomotion in real-world terrains and smooth transition between the two. Video of the robot during field testing is currently posted at <http://faculty.nps.edu/ravi/BioRobotics/Projects.htm>.

Fully operational field-ready versions of the vehicle are also presently under development. Targeted applications include a wide range of search and rescue, safety and security mission scenarios [52]. Rescue, fire, or police units will clearly benefit from a small robotic vehicle easily transported and deployed by the unit to provide situational awareness in specific areas. Another application of a vehicle capable of flight and ground movement would be in detection of dangerous or illegal substances. While a mono-modal unmanned aerial vehicle (UAV) might be capable of identifying the existence of potential threats from a distance, closer inspection is required to evaluate the validity of the threat. A small vehicle with the ability to land near and walk up to the location or object in question would allow an operator to accurately determine the presence or absence of harmful or dangerous substances. A scalable family of vehicles with multiple modes of locomotion is envisioned in future work based on the paradigms established in this research.

Acknowledgments This work was supported by the Air Force Research Laboratories Munitions Research Directorate (under contracts FA8651-04-C-0234 and FA8651-05-C-0097) and by the Naval Postgraduate School (NPS)/USSOCOM Field Experimentation Cooperative Program. The authors would like to acknowledge the program support directors Dr. David Netzer of the Naval Postgraduate School and Chris Perry and Jeffery Wagner at Us Air Force Research Laboratories for technical and mission planning insights. Dr. Kevin Jones provided assistance in sensor placement and piloting/performance research. Baron Johnson and Daniel Claxton made significant contributions including vehicle design and flight testing. Michael Sytsma, Michael Morton, and the University of Florida MAV group also contributed to the development, testing, and analysis of MALV II.

References

1. Ifju, P.G., Ettinger, S., Jenkins, D.A., Lian, Y., Shyy, W., Waszak, M.R.: Flexible-Wing-Based Micro Air Vehicles, 40th AIAA Aerospace Sciences Meeting, Reno, NV AIAA 2002-0705 (January 2002)
2. Morrey, J.M., Lambrecht, B., Horschler, A.D., Ritzmann, R.E., and Quinn, R.D.: Highly Mobile and Robust Small Quadruped Robots. IEEE Int. Conf. On Intelligent Robots and Systems (IROS'03), Las Vegas, Nevada, Vol. 1, pp. 82–87 (2003)
3. Morasso, P., Bottaro, A., Casadio, M., Sanguineti, V.: Pre-flexes and internal models in biomimetic robot systems. *Cognitive Process* 6, 25–36 (2005)
4. Alexander, R.McN.: Three Uses for Springs in Legged Locomotion. *International Journal of Robotics Research* 9, 2 (1990)
5. Shyy, W., Berg, M., Ljungqvist, D.: Flapping and Flexible Wings for Biological and Micro Vehicles. *Process in Aerospace Sciences* 35(5), 455–506 (1999)
6. Loeb, G.E., Brown, I.E., Cheng, E.J.: A hierarchical foundation for models of sensorimotor control. *Experimental Brain Research* 126, 1–18 (1999)
7. Jindrich, D.L., Full, R.J.: Dynamic stabilization of rapid hexapedal locomotion. *Journal of Experimental Biology* 205, 2803–2823 (2002)
8. Brown, I.E., Loeb, G.E.: A reductionist approach to creating and using neuromusculoskeletal models. In: J.M. Winters, P.E. Crago (eds.) *Biomechanics and neural control of movement*. Springer, Berlin Heidelberg New York, pp. 148–163 (1997)
9. Quinn, R.D., Nelson, G.M., Ritzmann, R.E., Bachmann, R.J., Kingsley, D.A., Offi, J.T., Allen, T.J.: Parallel Strategies For Implementing Biological Principles Into Mobile Robots. *International Journal of Robotics Research* 22(3), 169–186 (2003)
10. Saranli, U., Buehler, M., Koditschek, D.: RHex a simple and highly mobile hexapod robot. *International Journal of Robotics Research* 20(7), 616–631 (2001)
11. Stoeter, S.A., Rybski, P.E., Gini, M., Papanikolopoulos, N.: Autonomous Stair-Hopping with Scout Robots. *Proceedings of the IEEE International Conference on Intelligent Robots and Systems (IROS'02)*, pp. 721–726, Lausanne, Switzerland (September/October 2002)
12. Morrey, J.M., Lambrecht, B., Horschler, A.D., Ritzmann, R.E., Quinn, R.D.: Highly Mobile and Robust Small Quadruped Robots. *IEEE International Conference on Intelligent Robots and Systems (IROS 2003)*, Las Vegas (2003)
13. Kovac, M., Fuchs, M., Guignard, A., Zufferey, J.-C., Floreano, D.: A miniature 7 g jumping robot. *Proceedings of the IEEE International Conference on Robotics and Automation (ICRA'2008)*, pp. 373–378, (2008)
14. Daltorio K.A., Gorb, S., Peressadko, A., Horschler, A.D., Ritzmann, R.E., Quinn, R.D.: A Robot that Climbs Walls using Micro-structured Polymer Feet. *International Conference on Climbing and Walking Robots (CLAWAR)*, London, U.K. (September 13–15, 2005)
15. Kim, S., Asbeck, A., Provancher, W., Cutkosky, M.R.: SpinybotII: Climbing Hard Walls with Compliant Microspines. *Proceedings of the IEEE International Conference on Autonomous Robots*, Seattle, WA (July, 18–20, 2005)
16. K-TEAM SA HEADQUARTERS SWITZERLAND Chemin du Vuasset, CP 111, 1028 Préverenges, SWITZERLAND
17. Bererton, C., Navarro-Serment, L.E., Grabowski, R., Paredis, C.J.J., Khosla, P.K.: Millibots: Small Distributed Robots for Surveillance and Mapping. *Government Microcircuit Applications Conference*, pp. 20–23 (March 2000)
18. Fukui, R., Torii, A., Ueda, A.: Micro robot actuated by rapid deformation of piezoelectric elements. *Proceedings 2001 International Symposium on Micromechatronics and Human Science*, (MHS 2001), pp 117–22 (2001)
19. Birch, M.C., Quinn, R.D., Ritzmann, R.E., Pollack, A.J., Phillips, S.M.: Micro-robots inspired by crickets. *Proceedings of Climbing and Walking Robots Conference (CLAWAR'02)*. Paris, France (2002)
20. Clark, J.E., Cham, J.G., Bailey, S.A., Froehlich, E.M., Nahata, P.K., Full, R.J., Cutkosky, M.R.: Biomimetic design and fabrication of a hexapedal running robot. *Proceedings 2001 ICRA. IEEE International Conference on Robotics and Automation* 4, 3643–3649 (2001)
21. Allen, T.J., Quinn, R.D., Bachmann, R.J., Ritzmann, R.E.: Abstracted Biological Principles Applied with Reduced Actuation Improve Mobility of Legged Vehicles. *Proceedings of IEEE International Conference on Intelligent Robots and Systems (IROS '03)*, V.2, pp. 1370–1375. Las Vegas, USA (2003)
22. Morrey, J.M., Horschler, A.D., Didona, N., Lambrecht, B., Ritzmann, R.E., Quinn, R.D.: Increasing Small Robot Mobility Via Abstracted Biological Inspiration. *IEEE International Conference on Robotics and Automation (ICRA'03) Video Proceedings*. Taiwan (2003)
23. Kim, S., Clark, J.E., Cutkosky, M.R.: iSprawl: Design and Tuning for High Speed Autonomous Open Loop Running. *International Journal of Robotics Research* 25(9), 903–912 (2006)
24. Grasmeyer, J.M., Keennon, M.T.: Development of the Black Widow Micro Air Vehicle. *AIAA Chapter No.* 2001-0127 (2001)
25. Morris, S., Holden, M.: Design of Micro Air Vehicles and Flight Test Validation. *Proceeding of the Fixed, Flapping*

- and Rotary Wing Vehicles at Very Low Reynolds Numbers, pp. 153–176 (2000)
26. *Frontiers of Engineering: Reports on Leading Edge Engineering*, 2001 NAE Symposium on Frontiers of Engineering, National Academy of Engineering, p. 12 (2002)
 27. Ellington, C.P.: The Aerodynamics of Hovering Flight. *Philosophical Transactions of the Royal Society of London* **305**(1122), 1–181 (1984)
 28. Frampton, K.D., Goldfarb, M., Monopoli, D., Cveticanin, D.: Passive Aeroelastic Tailoring for Optimal Flapping Wings. *Proceeding of the Fixed, Flapping and Rotary Wing Vehicles at Very Low Reynolds Numbers*, pp. 26–33 (2000)
 29. Jones, K.D., Duggan, S.J., Platzer, M.F.: Flapping-Wing Propulsion for a Micro Air Vehicle. AIAA Chapter No. 2001–0126 (2001)
 30. Jones, K.D., Bradshaw, C.J., Papadopoulos, J., Platzer, M.F.: Improved Performance and Control of Flapping-Wing Propelled Micro Air Vehicles. 42nd AIAA Aerospace Sciences Meeting and Exhibit, AIAA Chapter 2004–0399, Reno, Nevada (January 5–8, 2004)
 31. Lentink, D., Bradshaw, N., Jongerius, S.R.: Novel micro aircraft inspired by insect flight. *Comparative Biochemistry and Physiology, Part A* **146**, S133–S134 (2007)
 32. Waszak, M.R., Jenkins, L.N., Ifju, P.G.: Stability and Control Properties of an Aeroelastic Fixed Wing Micro Aerial Vehicle. AIAA Chapter no. 2001–4005 (2001).
 33. Shyy, W.: *Computational Modeling for Fluid Flow and Interfacial Transport*. Elsevier, Amsterdam, The Netherlands (1994) (revised printing 1997).
 34. Shyy, W., Thakur, S.S., Ouyang, H., Liu, J., Bloesch, E.: *Computational Techniques for Complex Transport Phenomena*. Cambridge University Press, New York (1997)
 35. Shyy, W., Udaykumar, H.S., Rao, M.M., Smith, R.W.: *Computational Fluid Dynamics with Moving Boundaries*. Taylor & Francis, Washington, DC (1996) (revised printing 1997 & 1998).
 36. Smith, R.W., Shyy, W.: Computational Model of Flexible Membrane Wings in Steady Laminar Flow. *AIAA Journal* **33**(10), 1769–1777 (1995)
 37. Jenkins D.A., Shyy, W., Sloan, J., Klevebring, F., Nilsson, M.: Airfoil Performance at Low Reynolds Numbers for Micro Air Vehicle Applications. Thirteenth Bristol International RPV/UAV Conference, University of Bristol (1998)
 38. Ifju, P.G., Ettinger, S., Jenkins, D.A., Martinez, L.: Composite Materials for Micro Air Vehicles. *Proceeding for the SAMPE Annual Conference*, Long Beach CA (May 6–10, 2001)
 39. Jenkins, D.A., Ifju, P.G., Abdulrahim, M., Olipra, S.: Assessment of the Controllability of Micro Air Vehicles. *Micro Air Vehicle Conference*, Bristol England (April 2001)
 40. Ettinger, S.M., Nechyba, M.C., Ifju, P.G., Waszak, M.: Vision-Guided Flight Stability and Control for Micro Air Vehicles. *Proceedings of the IEEE International Conference on Intelligent Robots and Systems* **3**, 2134–2140 (2002)
 41. Zufferey, J.-C., Klapotocz, A., Beyeler, A., Nicoud, J.-D., Floreano, D.: A 10-gram Vision-based Flying Robot. *Advanced Robotics* **21**(14), 1671–1684 (2007)
 42. Lachat, D., Crespi, A., Ijspeert, A.J.: Boxybot: A Swimming and Crawling Fish Robot Controlled by a Central Pattern Generator. *Proceedings of The First IEEE/RAS-EMBS International Conference on Biomedical Robotics and Biomechatronics (BioRob 2006)* **1**, 643–648
 43. Georgiadis, C., German, A., Hogue, A., Liu, H., Prahacs, C., Ripsman, A., Sim, R., Torres, L.-A., Zhang, P., Buehler, M., Dudek, G., Jenkin, M., Milios, E.: AQUA: An Aquatic Walking Robot. *Proceedings of IEEE/RSJ International Conference on Intelligent Robots and Systems, IROS 2004*, Sendai, Japan (September 28–October 2, 2004)
 44. Ijspeert, A., Crespi, A., Ryczko, D., Cabelguen, J.-M.: From swimming to walking with a salamander robot driven by a spinal cord model. *Science* **315**(5817), 1416–1420 (2007)
 45. Ayers, J., Davis, J.L., Rudolph, A. (eds.): *Neurotechnology for Biomimetic Robots*. The MIT Press, pp. 481–509 (2002)
 46. Michelson, R., Helmick, D., Reece, S., Amareno, C.: A Reciprocating Chemical Muscle (RCM) for Micro Air Vehicle “Entomopter” Flight. AUVSI’97, *Proceedings of the Association for Unmanned Vehicle Systems International* (July 1997)
 47. Watson, J.T., Ritzmann, R.E., Zill, S.N., Pollack, A.J.: Control of obstacle climbing in the cockroach, *Blaberus discoidalis*: I. Kinematics. *Journal of Comparative Physiology* **188**, 39–53 (2002)
 48. Mueller, T.J. (ed.): *Proceedings of the Conference on Fixed, Flapping and Rotary Wing Vehicles at Very Low Reynolds Numbers*, Notre Dame University, Indiana (June 5–7, 2000)
 49. Mueller, T.J.: The Influence of Laminar Separation and Transition on Low Reynold’s Number Airfoil Hysteresis. *Journal of Aircraft* **22**, 763–770 (1985)
 50. Pringle, J.W.S.: *Insect Flight*. Cambridge University Press, Cambridge (1957)
 51. Ritzmann, R.E., Fournier, C.R., Pollack, A.J.: Morphological and physiological identification of motor neurons innervating flight musculature in the cockroach, *Periplaneta Americana*. *Journal of Experimental Zoology* **225**, 347–356 (1983)
 52. Boria F.J., Bachmann, R.J., Ifju, P.G., Quinn, R.D., Vaidyanathan, R., Perry, C., Wagener, J.: A Sensor Platform Capable of Aerial and Terrestrial Locomotion. *Proceedings of IEEE/RSJ 2005 International Conference on Intelligent Robots and Systems (IROS2005)*, Edmonton, Alberta, Canada, pp. 2–6 (August 2005)
 53. Lambrecht, B.G.A., Horschler, A.D., Quinn, R.D.: A Small Insect Inspired Robot that Runs and Jumps. *Proceeding of the IEEE International Conference on Robotics and Automation (ICRA ’05)*, Barcelona, Spain (2005)
 54. Procerus Technologies (<http://www.procerusuav.com/>), Kestrel Installation and Configuration Guide (May 2006)
 55. Bachmann, R.J., Boria, F.J., Ifju, P.G., Quinn, R.D., Kline, J.E., Vaidyanathan, R.: Utility of a Sensor Platform Capable of Aerial and Terrestrial Locomotion. *Proceedings of the IEEE/ASME International Conference on Advanced Intelligent Mechatronics (AIM2005)*, Monterey California (July, 2005)